Dynamic Analysis of Planing Hulls in the Vertical Plane

Richard H. Akers[1]

The problem of predicting the forces acting on planing vessels and the resulting motions of the vessels has resisted analysis. Researchers have attacked the problem by using semi-empirical methods, two-dimensional methods and fully three-dimensional methods. A summary of the current status, benefits and drawbacks of each approach will be presented. An algorithm for predicting planing motion and forces based on a two-dimensional strip theory will be discussed in detail. The method has been validated against model test data and has been found to be an accurate predictor of heave, pitch and roll position, velocity, and to a lesser degree, acceleration. The method can be used to predict hull panel pressures in irregular seas, and is an attractive alternative to conventional methods of predicting planing hull bottom loading.

INTRODUCTION

Naval architects have been designing high-speed planing craft for most of this century, but the problem of predicting the motion of these craft has proven to be extremely difficult. If the problem of predicting planing craft motion is treated as a fully three-dimensional problem, the complexity makes the problem virtually intractable with today's level of understanding. If the problem is treated with semi-empirical methods, then the results are only valid within the range of data used to create the model.

In this paper a two-dimensional method proposed by Zarnick (1978) will be reviewed in detail. The method serves to bridge some of the deficiencies of the empirical methods, while remaining simple enough to be implemented on personal computers. The two-dimensional method is extended to predict dynamic panel pressures, and offers an alternative to the empirical structural design methods used by most designers today.

NUMERICAL METHODS FOR DYNAMIC ANALYSIS

Surface craft derive their lift from the hydrostatic displacement of water and from the dynamic momentum change in the water below the vessel. At low speeds the lift is primarily due to hydrostatic forces. As speed increases hydrodynamic lift increases, the vessel rises out of the water, and hydrostatic lift decreases. Most numerical methods assume that the forces acting on a planing craft can be separated into hydrostatic and hydrodynamic forces, and that the two can be treated independently.

Semi-Empirical Methods

A number of methods exist which combine first principle physics and empirical measurements to predict the speed-power relationships for planing hulls. The most popular method was developed by Savitsky (1964) and refined in Savitsky and Brown (1976). In Savitsky's long form method, the designer iterates through a series of steps to predict the running trim and draft and the required thrust for their planing hulls.

In the following calculations a value of trim τ is chosen, the moment M is calculated using the formulas listed in Table 1, and τ is adjusted until the moment M is 0, thus satisfying the equations of static equilibrium. The result is the running attitude and power requirement for a prismatic planing hull with constant deadrise β. In Table 1 the calculations labeled Empirical are curve-fit approximations to measured data.

The major advantages to Savitsky's method are that it is simple to perform and that for many common hullforms it is accurate.

There are a number of disadvantages to Savitsky's method, however. Hulls that have variable deadrise either longitudinally or transversely can not be modeled directly with Savitsky's method. Further, the method is quasi-static and does not directly predict transient behavior. Finally, the method lumps all forces into a series of empirical relationships so point or panel hydrodynamic loads cannot be predicted using the method.

Calculate	**Source**	**Type**
F_B, Beam Froude Number	F_B=V/sqrt(g*B)	*Physics*
$C_{L\beta}$, Lift coeff. with deadrise	$C_{L\beta}=W/(1/2\rho V^2 B^2)$	*Physics*

[1] Ship Motion Associates, Portland, Maine.

Presented at the April 29, 1999 meeting of the New England Section of THE SOCIETY OF NAVAL ARCHITECTS AND MARINE ENGINEERS.

C_{L0}, Flat plate lift coeff.		*Empirical*
λ, Mean wetted length ratio		*Empirical*
C_{Ld}, Dynamic lift coeff.		*Empirical*
V_m, Bottom velocity	V_m=V sqrt(1-C_{Ld}/(cos τ))	*Physics*
R_n, Reynolds Number	R_n=ρV_m(Bλ)/μ	*Physics*
C_F, Coeff. of Friction	Prandtl-Schlichting line	*Empirical*
ΔC_F, ATTC Roughness		*Empirical*
S_F, Wetted area	S_F=λB^2/cos β	*Physics*
D_F, Friction drag	D_F=1/ρV_m2$S_F$$C_F$	*Empirical*
D, Drag	D=W tan τ+D_F/ cos τ	*Physics*
T, Prop thrust	T=(W sinτ+D_F)/ cos ε	*Physics*
N, Normal Force	N=W cos(τε) -D_F sin □)/cos ε	*Physics*
L_m, Mean wetted length	L_m=(h/sin τ - B/2π tan β/tan τ)	*Physics*
L_p, Center of pressure		*Empirical*
c, Normal force moment arm	c=LCG-L_p	*Physics*
a, Friction drag moment arm		*Empirical*
M, Pitching moment	M=Tf-Nc-D_Fa	*Physics*
Pe, Effective power	Pe=DV	*Physics*

Table 1 Formulas in Savitsky's Method

Two-Dimensional Planing Theory

Planing hulls create lift by dynamically displacing water. At high speeds the perturbation water velocity in the surge direction of the vessel is negligible. As a result the perturbation flow can be approximated by the sum of a series of two-dimensional sections. Individual sections resemble impacting wedges.

E. E. Zarnick (1978) formulated a mathematical model of forces acting on a planing craft. Zarnick's method assumes that wavelengths will be large with respect to the craft's length and that wave slopes will be small. Zarnick's method will be discussed further in the section entitled *Low Aspect Ratio Strip Theory*.

Three-Dimensional Panel Methods

Panel methods solve for fluid flow around an object by assuming that the fluid is inviscid, irrotational and incompressible. In such a region a velocity potential exists that is described by Laplace's equation:

$$\nabla^2\Phi = 0$$

For a submerged body the velocity component normal to the body's surface and to the free surface must be zero, so the following boundary conditions apply:

$$\nabla\Phi \bullet \vec{n}_b = 0$$

$$\nabla\Phi \bullet \vec{n}_\zeta \Big|_{\zeta=0} = 0$$

Any perturbation in the free stream or relative velocity $\vec{v}$ created by the object should decay far from the object, so an additional boundary condition is:

$$\lim_{r\to\infty}(\nabla\Phi) = \vec{v}$$

Elementary solutions to Laplace's equation include point sources and doublets, and vortices. Three-dimensional versions of these elementary types located at the origin can be described by the following:

Point Sources	$\Phi = \frac{\sigma}{r4\pi}$
Point Doublets	$\Phi = \frac{\mu}{4\pi}\vec{n} \bullet \nabla\left(\frac{1}{r}\right) = -\frac{\partial}{\partial n}\Phi_{source}$
Vortices (2-D version)	$\Phi = -\frac{\Gamma}{4\pi}\theta + \text{constant}$

Panel methods take advantage of the fact that polynomial sums of these elementary solutions also satisfy Laplace's equation. In panel methods the vessel's surface is replaced with a set of panels, and each panel is assigned one or more of these elementary solutions. Furthermore, each panel is assigned a control location or "collocation point" for which the solid body boundary condition must be met (refer to Figure 1).

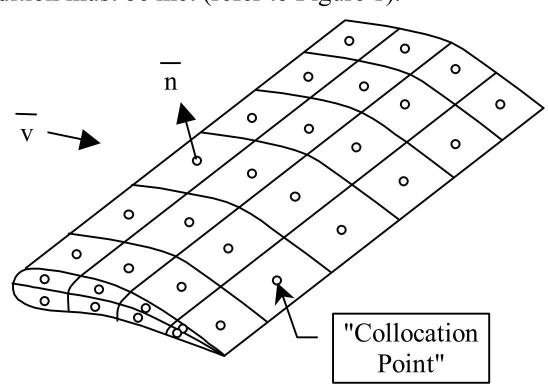

Figure 1 Approximation of Body Surface by Panel Elements

Nomenclature

B = Beam (assumed constant)
C_{BF} = Buoyancy force coefficient
C_{BM} = Buoyancy moment coefficient
$C_{D,c}$ = Crossflow (transverse) drag coefficient
C_F = Overall friction coefficient
CG = Center of gravity (location)
C_Δ = Loading coefficient $= \Delta/\rho g B^3$
C_λ = Wavelength coefficient, $= L/\lambda\ (C_\Delta/(L/B)^2)^{1/3}$
F_B = Buoyancy force
F_D = Total drag force in $-\xi$ direction
F_N = Force normal to boat hull, positive down
F_X = Force in X direction (global coordinates), positive forward
F_Z = Force in Z direction (global coordinates), positive down
F_θ = Moment in pitch direction, positive bow-up
H = Wave height
I = Pitch moment of inertia
L = Vessel length
M = Mass of vessel
M_a = Total added mass
Q_a = Total added mass moment of inertia
R_W = Total mean resistance in waves
T = Thrust force (magnitude)
T_X = Thrust force component in X direction
T_Z = Thrust force component in Z direction
$U, \dot{U}$ = Velocity, acceleration in ξ direction
$V, \dot{V}$ = Velocity, acceleration in ζ direction
V_K = Velocity in knots
W = Weight of vessel
a = Sectional area
b = Sectional half-beam
f_D = Sectional friction drag
g = Acceleration of gravity
g_i = Sectional wetted girth
h = Peak-to-peak heave response
m_a = Sectional added mass
$\dot{m}_a$ = Time-derivative of sectional added mass
$\vec{n}, \vec{n}_b, \vec{n}_\zeta$ = Normal vector, normal to body, normal to free surface
$\overline{p}_{1/10}$ = Ave. of 1/10 highest pressures
$\tilde{p}_{1/1000}$ = Most probable peak pressure
$\vec{v}$ = Relative velocity vector between undisturbed fluid and body (panel method)
v_i = Sectional velocity (calculated from forward "cant" of surface normal)
$x, \dot{x}, \ddot{x}$ = Longitudinal position, velocity and acceleration in surge (longitudinal) direction, global coordinates
x_B = Distance from CG to center of buoyancy
x_C = Distance from CG to center of normal force
x_D = Distance from CG to center of action for drag force
x_P = Distance from CG to thrust vector
$z, \dot{z}, \ddot{z}$ = Vertical position, velocity and acceleration in heave direction, global coordinates, positive downwards
Δ, Δ_{LT} = Displacement, displacement in long tons
Φ = Velocity potential for panel method
Γ = Vortex circulation
β = Deadrise of prismatic hull
λ = Water wavelength
μ = Doublet strength
θ_P = Peak-to-peak pitch response, radians
$\theta, \dot{\theta}, \ddot{\theta}$ = Pitch position, velocity, acceleration, positive bow-up
ρ = Density of water
σ = Source strength
τ = Trim angle, radians
ξ = Longitudinal boat coordinate, measured positive forward from CG
ζ = Vertical boat coordinate, measured positive down from CG; also free surface location in global coordinates for panel method

A panel method solver must find a combination of source strengths σ, doublet strengths μ, or vortex circulations Γ such that the boundary conditions are met at the surface, at the object body and at the far field. Once all of the panel strengths are known velocities and pressures can be calculated for each panel. There are a number of difficulties with using panel methods to predict the flow around planing hulls. First, the free surface location ζ is a function of the *solution* of the problem. That is, iterative solutions are required to estimate the free surface location as a function of the fluid velocity potential and to estimate the fluid velocity potential as a function of the free surface location.

A second problem with panel methods is that the geometry of the problem is a function of the solution to the problem. That is, the wetted surface of the planing craft depends on the separation of the water at the chine and transom. This means that the location of the panels and their resulting normal vectors is a function of the fluid velocity potential, which is a function of the geometry. Again, iterative or time-stepping methods must be employed.

A third problem with panel methods is that velocity potentials cannot be used directly to model viscous boundary layers or pressures from spray jets. Empirical methods are typically used to create effective geometries that take into account boundary layers, and to model spray pressures.

LOW ASPECT RATIO STRIP THEORY

Zarnick (1978), following the work of Martin (1976), developed a mathematical formulation for the instantaneous forces on a planing craft. In Zarnick's method a planing craft is modeled as a series of strips or impacting wedges. Zarnick derived the normal hydrodynamic force per unit length as:

$$f = -\left\{ \frac{D}{Dt}\left(m_a V\right) + C_{D,c}\rho b V^2 \right\}$$

$$\text{where } \frac{D}{Dt}\left(m_a V\right) = m_a \dot{V} + \dot{m}_a V - \frac{\partial}{\partial \xi}\left(m_a V\right)\frac{d\xi}{dt}$$

A characteristic outward normal vector $\vec{n}$ is defined for each strip and submergence (Figure 2). The normal vector is arbitrarily defined at the longitudinal midpoint of the strip and at a height of 2/3 of the submergence above the keel line. The instantaneous deadrise angle is defined as the angle of the normal with respect to the baseplane as seen in the body plan view.

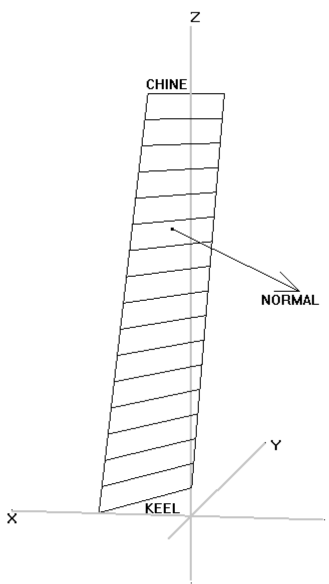

Figure 2 Normal Vector for Strip near Bow

Sectional added mass is modeled as if it were an impacting wedge:

$$m_a = k_a \frac{\pi}{2}\rho b^2 \text{ and } \dot{m}_a = k_a \pi \rho b \dot{b}$$

where k_a is an added mass coefficient. In the preceding equations the time-dependency of the added mass coefficient k_a is neglected. Zarnick used the value k_a = 1.0, which is taken from the derivation of Wagner (1932).

Vorus (1996) suggested that an added mass coefficient that is dependent on the deadrise angle might be more appropriate. Figure 3 is a plot of equivalent added mass coefficients taken from a variety of sources. Most modern sources agree that the added mass coefficient is deadrise-dependent, so the following formula is used in this analysis:

$$k_a = \frac{\pi^2}{4}\left(1 - \frac{\beta}{90} * 0.4 * \left(1 - KAR\right)\right)$$

where KAR is an added mass correction factor. Using KAR=1.0 is equivalent to using the added mass coefficient of Wagner, while using KAR=0.0 roughly matches the added mass coefficient curve of Vorus.

Since the horizontal component w_X of the wave orbital velocity is considered small with respect to $\dot{x}_{CG}$ only the vertical component w_Z is included. The boat relative velocities with the vertical wave component included are:

$$U = \dot{x}_{CG} * \cos(\theta) - \left(\dot{z} - w_Z\right) * \sin(\theta)$$

$$V = \dot{x}_{CG} * \sin(\theta) + \left(\dot{z} - w_Z\right) * \cos(\theta) - \dot{\theta}\xi$$

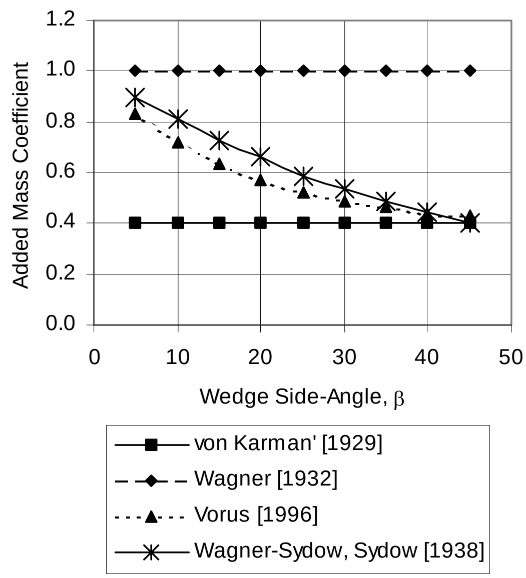

Figure 3 Added Mass Coefficient for Impacting Wedges, ka

Hydrostatic forces and moments must be included in the analysis, but are difficult to predict. Water rise at the bow of a planing vessel increases hydrostatic lift, flow separation at the stern decreases hydrostatic lift, and both cause an increase in pitching moment. These effects are speed dependent, and there is no single factor that can be used to correct the hydrostatics calculations for flow separation. In his work on rectangular planing surfaces, Shuford (1958) suggested that hydrostatic buoyancy should be halved in a dynamic simulation in order to achieve the correct total lift force. Zarnick (1978) found that use of an additional factor of one-half for the hydrostatic moment resulted in an accurate trim angle. In the following equations coefficients C_{BF} and C_{BM} correct the vertical force and pitching moment. These coefficients can be set to 0.5 based upon the recommendation of Shuford and Zarnick, or they can be set empirically so that simulation results match tank test results.

A summary of the forces acting on the planing craft is:

$$F_N = \int_l \left\{ m_a \dot{V} + \dot{m}_a V - U \frac{\partial m_a V}{\partial \xi} + C_{D,c} \rho b V^2 \right\} d\xi$$

$$F_Z = -F_N * \cos(\theta) - \int_l \rho g C_{BF} a d\xi$$

$$F_X = -F_N * \sin(\theta)$$

$$F_\theta = \int_l \{ m_a \dot{V} + \dot{m}_a V - U \frac{\partial m_a V}{\partial \xi} + C_{D,c} \rho b V^2 - \rho g C_{BM} a * \cos(\theta) \} \xi \, d\xi$$

The vertical force F_Z is expanded as follows:

$$F_Z = -F_N * \cos(\theta) - \int_l \rho g C_{BF} A d\xi$$

$$= -\int_l \{ (m_a \dot{V} + \dot{m}_a V - U \frac{\partial m_a V}{\partial \xi}) \cos(\theta) + C_{D,c} \rho b V^2 \cos(\theta) + \rho g C_{BF} a \} \, d\xi$$

The time derivatives and partial derivatives of the boat-coordinate velocities are:

$$\dot{V} = \ddot{x}_{CG} \sin(\theta) - \ddot{\theta}\xi + \ddot{z}_{CG} \cos(\theta) - \dot{w}_Z \cos(\theta) + \dot{\theta}(\dot{x}_{CG} \cos(\theta) - \dot{z}_{CG} \sin(\theta)) + w_Z \dot{\theta} \sin(\theta)$$

$$\frac{\partial V}{\partial \xi} = -\dot{\theta} - \frac{\partial w_Z}{\partial \xi} \cos(\theta)$$

$$\frac{\partial U}{\partial \xi} = \frac{\partial w_Z}{\partial \xi} \sin(\theta)$$

The vertical component of the wave orbital velocity can be described by:

$$\frac{dw_Z}{dt} = \dot{w}_Z - U \frac{\partial w_Z}{\partial \xi}$$

$$\text{so } \dot{w}_Z = \frac{dw_Z}{dt} + U \frac{\partial w_Z}{\partial \xi}$$

Using integration by parts one can avoid taking the integral of the partial derivative of the added mass with respect to ξ:

$$\int_l m_a \frac{\partial UV}{\partial \xi} d\xi = -\int_l UV \frac{\partial m_a}{\partial \xi} d\xi + UVm_a \Big|_{bow}^{stern}$$

so

$$\int_l UV \frac{\partial m_a}{\partial \xi} d\xi = -UVm_a \Big|_{stern} - \int_l m_a \frac{\partial UV}{\partial \xi} d\xi$$

Making these substitutions and simplifying yields:

$$\begin{aligned} F_Z = \{ & -M_a \cos(\theta) \ddot{z}_{CG} - M_a \sin(\theta) \ddot{x}_{CG} + Q_a \ddot{\theta} \\ & + M_a \dot{\theta} (\dot{z}_{CG} \sin(\theta) - \dot{x}_{CG} \cos(\theta)) \\ & + \int_l m_a \frac{dw_Z}{dt} \cos(\theta) d\xi - \int_l m_a w_Z \dot{\theta} \sin(\theta) d\xi \\ & - \int_l m_a V \frac{\partial w_Z}{\partial \xi} \sin(\theta) d\xi + \int_l m_a U \frac{\partial w_Z}{\partial \xi} \cos(\theta) d\xi \\ & - UVm_a \Big|_{stern} - \int_l V \dot{m}_a d\xi \\ & - \rho \int_l C_{D,c} b V^2 d\xi \} * \cos(\theta) - \int_l \rho g C_{BF} a d\xi \end{aligned}$$

A similar analysis for the horizontal force and for the pitch moment yields:

$$\begin{aligned} F_x = \{ & -M_a \cos(\theta) \ddot{z}_{CG} - M_a \sin(\theta) \ddot{x}_{CG} + Q_a \ddot{\theta} \\ & + M_a \dot{\theta} (\dot{z}_{CG} \sin(\theta) - \dot{x}_{CG} \cos(\theta)) \\ & + \int_l m_a \frac{dw_Z}{dt} \cos(\theta) d\xi - \int_l m_a w_Z \dot{\theta} \sin(\theta) d\xi \\ & - \int_l m_a V \frac{\partial w_Z}{\partial \xi} \sin(\theta) d\xi + \int_l m_a U \frac{\partial w_Z}{\partial \xi} \cos(\theta) d\xi \\ & - UVm_a \Big|_{stern} - \int_l V \dot{m}_a d\xi \\ & - \rho \int_l C_{D,c} b V^2 d\xi \} * \sin(\theta) \end{aligned}$$

$$\begin{aligned} F_\theta = & -I_a \ddot{\theta} + Q_a \cos(\theta) \ddot{z}_{CG} \\ & - Q_a \dot{\theta} (\dot{z}_{CG} \sin(\theta) - \dot{x}_{CG} \cos(\theta)) \\ & - \int_l m_a \frac{dw_Z}{dt} \cos(\theta) \xi d\xi + \int_l m_a w_Z \dot{\theta} \sin(\theta) \xi d\xi \\ & + \int_l m_a V \frac{\partial w_Z}{\partial \xi} \sin(\theta) d\xi - \int_l m_a U \frac{\partial w_Z}{\partial \xi} \cos(\theta) d\xi \\ & + UVm_a \xi \Big|_{stern} + \int_l m_a UV d\xi \\ & + \int_l V \dot{m}_a \xi d\xi + \rho \int_l C_{D,c} b V^2 \xi d\xi \\ & - \int_l \rho g C_{BM} a \cos(\theta) \xi d\xi \end{aligned}$$

Solving Equations of Motion

The governing equations that determine the motion of a planing craft are:

$$\begin{aligned} M\ddot{x}_{CG} &= T_X - F_N \sin(\theta) - F_D \cos(\theta) \\ &= T_X + F_X - F_D \cos(\theta) \\ M\ddot{z}_{CG} &= T_Z - F_N \cos(\theta) - F_B + F_D \sin(\theta) + W \\ &= T_Z + F_Z + F_D \sin(\theta) + W \\ I\ddot{\theta} &= T * x_P + F_N * x_C - F_B * x_B - F_D * x_D \\ &= T * x_P + F_\theta - F_D * x_D \end{aligned}$$

The acceleration terms can be factored out of the sectional force and moment expressions:

$$
\begin{aligned}
F'_X &= F_X \text{ - (acceleration terms)} \\
&= M_a\dot{\theta}\left(\dot{z}_{CG}\sin(\theta) - \dot{x}_{CG}\cos(\theta)\right) \\
&\quad + \int_l m_a \frac{dw_Z}{dt}\cos(\theta)d\xi - \int_l m_a w_Z\dot{\theta}\sin(\theta)d\xi \\
&\quad - \int_l m_a V\frac{\partial w_Z}{\partial \xi}\sin(\theta)d\xi + \int_l m_a U\frac{\partial w_Z}{\partial \xi}\cos(\theta)d\xi \\
&\quad - UVm_a\big|_{stern} - \int_l V\dot{m}_a d\xi - \rho\int_l C_{D,c} bV^2 d\xi\} * \sin(\theta)
\end{aligned}
$$

$$
\begin{aligned}
F'_Z &= F_Z \text{ - (acceleration terms)} \\
&= M_a\dot{\theta}\left(\dot{z}_{CG}\sin(\theta) - \dot{x}_{CG}\cos(\theta)\right) \\
&\quad + M_a\dot{\theta}\left(\dot{z}_{CG}\sin(\theta) - \dot{x}_{CG}\cos(\theta)\right) \\
&\quad + \int_l m_a \frac{dw_Z}{dt}\cos(\theta)d\xi - \int_l m_a w_Z\dot{\theta}\sin(\theta)d\xi \\
&\quad - \int_l m_a V\frac{\partial w_Z}{\partial \xi}\sin(\theta)d\xi + \int_l m_a U\frac{\partial w_Z}{\partial \xi}\cos(\theta)d\xi \\
&\quad - UVm_a\big|_{stern} - \int_l V\dot{m}_a d\xi \\
&\quad - \rho\int_l C_{D,c} bV^2 d\xi\} * \cos(\theta) + \int_l \rho g C_{BF} a d\xi
\end{aligned}
$$

$$
\begin{aligned}
F'_\theta &= F_\theta - \text{(acceleration terms)} \\
&= -Q_a\dot{\theta}\left(\dot{z}_{CG}\sin(\theta) - \dot{x}_{CG}\cos(\theta)\right) \\
&\quad - \int_l m_a \frac{dw_Z}{dt}\cos(\theta)\xi d\xi + \int_l m_a w_Z\dot{\theta}\sin(\theta)\xi d\xi \\
&\quad + \int_l m_a V\frac{\partial w_Z}{\partial \xi}\sin(\theta)d\xi - \int_l m_a U\frac{\partial w_Z}{\partial \xi}\cos(\theta)d\xi \\
&\quad + UVm_a\xi\big|_{stern} + \int_l m_a UVd\xi + \int_l V\dot{m}_a \xi d\xi \\
&\quad + \rho\int_l C_{D,c} bV^2 \xi d\xi - \int_l \rho g C_{BM} a\cos(\theta)\xi d\xi
\end{aligned}
$$

Combining modified sectional force and moment expressions with the general equations of motion yields:

$$
\begin{vmatrix}
M + M_a\sin^2\theta & M_a\sin(\theta)\cos(\theta) & -Q_a\sin\theta \\
M_a\sin(\theta)\cos(\theta) & M + M_a\cos^2\theta & -Q_a\cos\theta \\
-Q_a\sin\theta & -Q_a\cos\theta & I + I_a
\end{vmatrix}
\times
\begin{vmatrix}
\ddot{x}_{CG} \\ \ddot{z}_{CG} \\ \ddot{\theta}
\end{vmatrix}
=
\begin{vmatrix}
T_X + F'_X - F_D\cos\theta \\
T_Z + F'_Z + F_D\sin\theta + W \\
T * x_P + F'_\theta - F_D * x_D
\end{vmatrix}
$$

A set of state variables $\dot{x}_{CG}, \dot{z}_{CG}, \dot{\theta}_{CG}$, x_{CG}, z_{CG}, and θ_{CG} are chosen. The matrix equation above can be written as $|A|\,\dot{\vec{x}} = \vec{f}$ where |A| is the mass matrix, $\dot{\vec{x}}$ is the derivative of the state variable vector $\left(\dot{x}_{CG}, \dot{z}_{CG}, \dot{\theta}_{CG}\right)$, and $\vec{f}$ is the right-hand side forcing function, which is itself a function of the state variables.

At each time step the matrix equation is solved for $\dot{\vec{x}} = |A|^{-1}\,\vec{f}$. The resulting equations are integrated to find the new value of the state variables $\dot{x}_{CG}, \dot{z}_{CG}$ and $\dot{\theta}_{CG}$, and the previous value of the state variables $\dot{x}_{CG}, \dot{z}_{CG}$ and $\dot{\theta}_{CG}$ are integrated to find the new value of the state variables x_{CG}, z_{CG}, and θ_{CG}.

Special attention is paid to the friction force F_D. At each time step the mean wetted length, the Reynolds Number, and a friction coefficient can be calculated. The friction coefficient is calculated using the Prandtl-Schlichting line. For most of the hull this friction coefficient will be valid, but for highly curved sections the water flow will be significantly greater than the nominal water flow past the hull. A sectional friction force is calculated as:

$$
f_D = \frac{1}{2} C_F \rho\, v_i^2 g_i
$$

where f_D = Sectional friction drag

C_F = Overall friction coefficient

v_i = Sectional velocity (calculated from forward "cant" of surface normal)

g_i = Sectional wetted girth

Validation in Calm Water and Regular Seas

The algorithm has been implemented in the form of a computer program called POWERSEA. POWERSEA runs on a personal computer equipped with the Windows 95, 98 or NT operating system. It is important to verify that the algorithm was implemented correctly, and to confirm that the algorithm as implemented does calculate the response of a vessel accurately. To verify the POWERSEA implementation of the strip-theory algorithm, simulations were performed on idealized hulls designed by Gerard Fridsma (1969) of the Davidson Laboratory of Stevens Institute of Technology. Fridsma constructed and tested a range of prismatic models (refer to Figure 4) at different speeds and in a range of regular seas.

As the POWERSEA program was designed to simulate planing hulls, only Fridsma's high speed tests could be duplicated. All of the tests shared the following characteristics:

Model Length	3.75	feet
Beam	0.75	feet
Speed/Length Ratio	6.0	knots/foot$^{1/2}$

The four test conditions simulated with POWERSEA correspond to the following Fridsma configurations:

Configuration	Wt (lb)	Deadrise β (degr/)	LCG (%L from Bow)
B	16.0	20	62.0
G	24.0	20	58.0
J	16.0	10	68.0
M	16.0	30	60.5

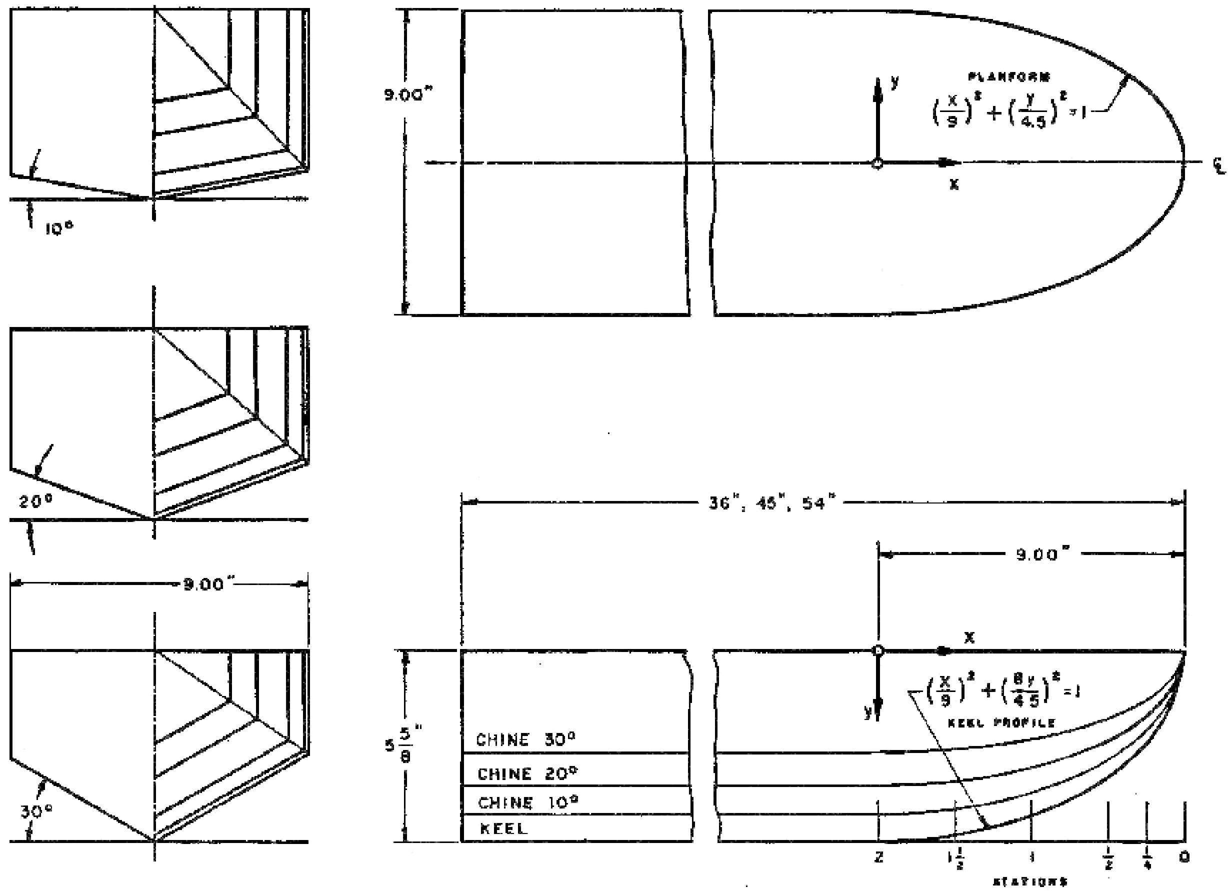

Figure 4 Lines of Prismatic Models, Fridsma (1969)

The results of POWERSEA simulations for calm water conditions are summarized in Table 2. By adjusting buoyancy coefficients C_{BF} and C_{BM} it is possible to reproduce Fridsma's calm water resistance and trim quite accurately. The notable exception is for configuration J, which has a low 10-degree deadrise angle.

	Design Trim Angle τ (degr.)		R_W/Δ		Buoyancy Coefficients	
	Fridsma	PWRS	Fridsma	PWRS	C_{BF}	C_{BM}
B	4.0	4.00	0.206	0.206	0.985	0.698
G	5.0	5.00	0.178	0.178	0.787	0.994
J	4.0	4.11	0.156	0.176	1.00	1.00
M	4.0	3.997	0.264	0.258	0.806	1.00

Table 2 Calm Water Performance

Fridsma observed very low resistance when testing configuration J, and it was not possible to adjust coefficients to match the measured resistance. This is possibly due to three-dimensional flows inherent with low deadrise planing surfaces that are not modeled properly in the POWERSEA strip theory algorithm.

Symbol/ Name	Definition	Use
C_Δ	$\Delta / \rho g b^3$	Load Coefficient
C_λ (Clambda)	$\frac{L}{\lambda} \sqrt[3]{\frac{C_\Delta}{(L/b)^2}}$	Non-dimensionalized Wavelength
Pitch RAO	$\theta_P / (2\pi H/\lambda)$	Non-dimensionalized Pitch Response
Heave RAO	h/H	Non-dimensionalized Heave
Resistance RAO	R_W/Δ	Total resistance

Table 3 Non-Dimensionalized Response Variables

After testing his models in calm water, Fridsma ran a series of tests in regular waves. Pitch, heave, resistance and acceleration were measured for each model in waves with a range of wavelengths. To present results that could be applied to a variety of vessels, Fridsma defined a set of non-dimensionalized response variables listed in Table 3.

A series of tests were run in waves with an amplitude of 1/2 inch and wavelengths as defined in Table 4.

λ/L	λ (feet)	C_λ (B, J, M)	C_λ (G)
1	3.75	0.290	0.332
1.5	5.0	0.193	0.221
2	7.5	0.145	0.166
3	10.25	0.097	0.111
4	15.0	0.072	0.083
6	20.5	0.048	0.055

Table 4 Fridsma's Normalized Wavelengths

Each configuration was tested with the suggested buoyancy coefficients of C_{BF}=0.5 and C_{BM}=0.5 (denoted as "Low Buoyancy" in the following figures), and also with the buoyancy coefficients listed in Table 2.

The pitch variable θ_P is defined as the average of the heights of the time-domain pitch data. This is calculated by finding the average of the crests, the average of the troughs, and summing the two figures. Likewise, the heave variable h is the average of the heights of the data. The acceleration response values are the RMS of the time-domain acceleration data. The resistance response is the mean of the predicted resistance.

Figure 5, Figure 10, Figure 15 and Figure 20 show the pitch response of each of the four configurations as a function of the non-dimensionalized wavelength C_λ. In all cases the pitch response tracked with Fridsma's experimental data quite well for short wavelengths (C_λ greater than 0.1 to 0.15).

For each combination of loading, deadrise, speed and amplitude there is at least one resonant wavelength. As can be seen in the figures, the theory predicts the wavelength of the resonant frequency quite accurately, but is less accurate in predicting the maximum amplitude of the pitch motion. At the resonant frequency there will be large motions, and possibly the algorithm needs to be extended to predict slamming and other three-dimensional phenomena.

For configurations G (high loading, Figure 10) and J (low deadrise, Figure 15) the best predictor of the peak pitch response amplitude is the version of the model with the default buoyancy coefficients. For configuration M (high deadrise, Figure 20) the best prediction occurs with the estimated, higher buoyancy coefficients.

Configuration J (Figure 15) shows a double resonant behavior. The cause of this behavior is that the vessel actually resonates with every other wave, rebounding over alternate waves. Simulating configuration J with the default buoyancy factors reproduces the double-resonant pitch and heave behavior quite accurately.

The heave response of these four configurations is plotted in Figure 6, Figure 11, Figure 16 and Figure 21. As for the pitch response, for higher values of C_λ (greater than 0.1 to 0.12) the algorithm tracks the response accurately. For configuration M, the high-deadrise case, the best predictor of the heave response amplitude is the model with the higher buoyancy coefficients. Otherwise, the best predictor of the dynamic heave response is the model with the default lower buoyancy coefficients.

The simulated RMS acceleration responses (Figure 7, Figure 8, Figure 12, Figure 13, Figure 17, Figure 18, Figure 22 and Figure 23) are reasonably accurate, although not quite as good as the simulated heave and pitch responses. The maximum acceleration values at the resonant conditions (which would be used for structural design purposes) are predicted within 20% or so by using the default buoyancy coefficients. For configuration M (high-deadrise, Figure 22 and Figure 23), the accelerations are over-predicted for both sets of buoyancy coefficients, although use of the larger estimated coefficients gives slightly better results.

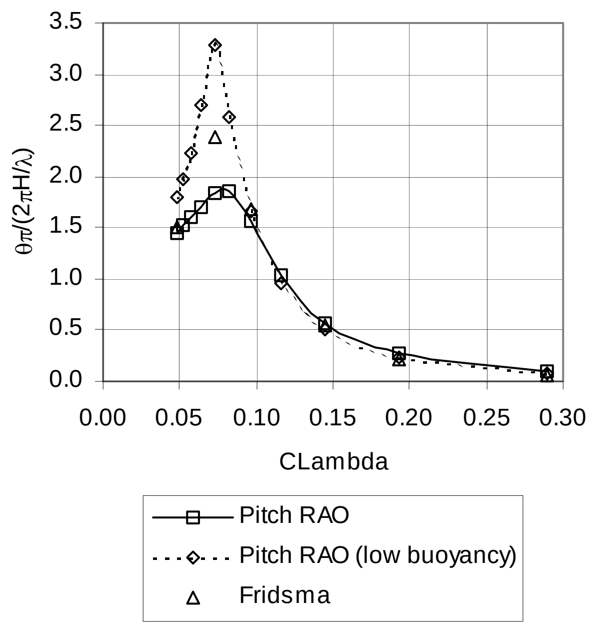

Figure 5 Config.B (16 lb, β=20): Pitch Response

The algorithm does a good job of predicting calm water resistance R_W, but tends to under predict the added resistance in waves. The resistance of all of configurations are best predicted by using the default buoyancy factors. The added resistance is predicted accurately for configuration M, the heavily-loaded case. The added-resistance of configuration J, the low deadrise case, is under predicted, probably because of the large motions at the resonant point.

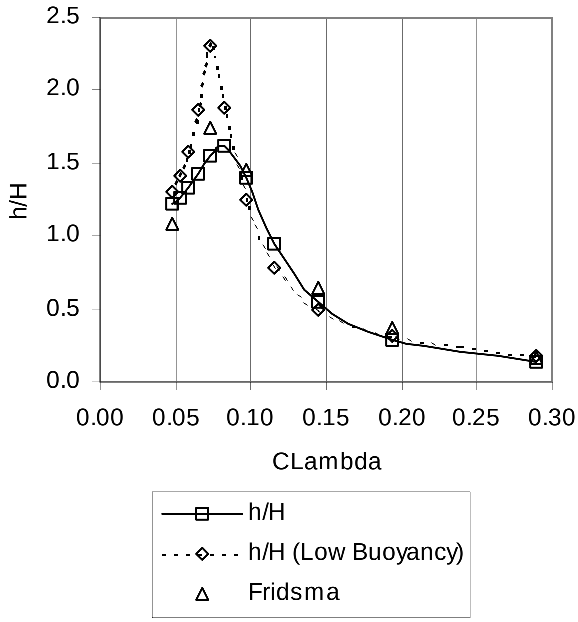

Figure 6 Config.B (16 lb, β=20): Heave Response

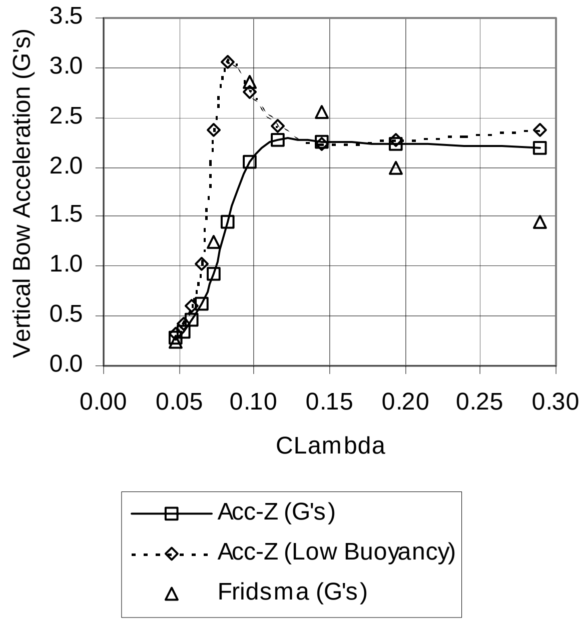

Figure 8 Config.B (16 lb, β=20): Vertical Acceleration at Bow

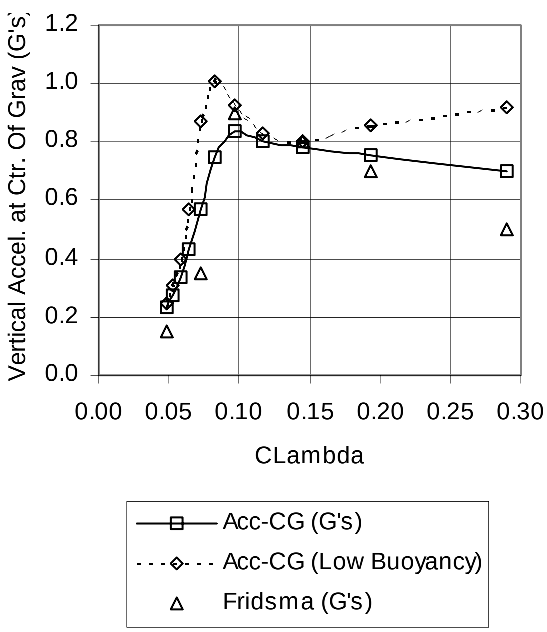

Figure 7 Config.B (16 lb, β=20): Vertical Acceleration at Center of Gravity

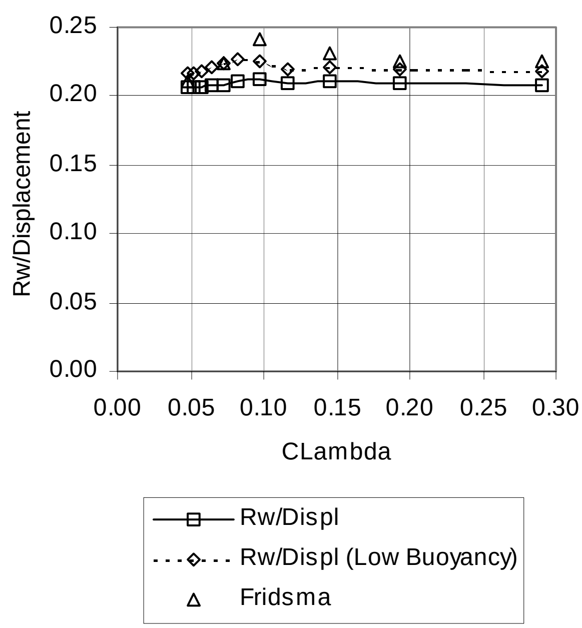

Figure 9 Config.B (16 lb, β=20): Resistance in Waves

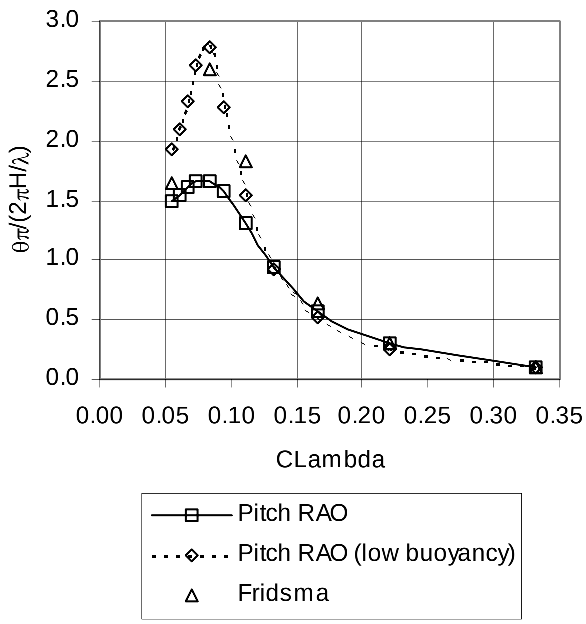

Figure 10 Config.G (24 lb, β=20): Pitch Response

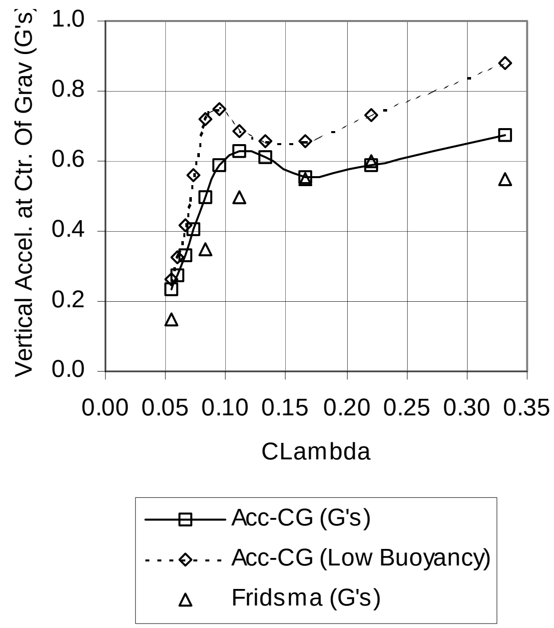

Figure 12 Config.G (24 lb, β=20): Vertical Acceleration at Center of Gravity

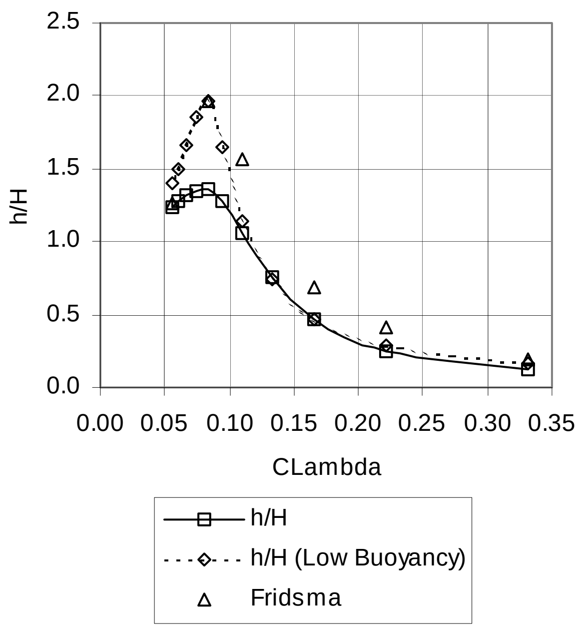

Figure 11 Config.G (24 lb, β=20): Heave Response

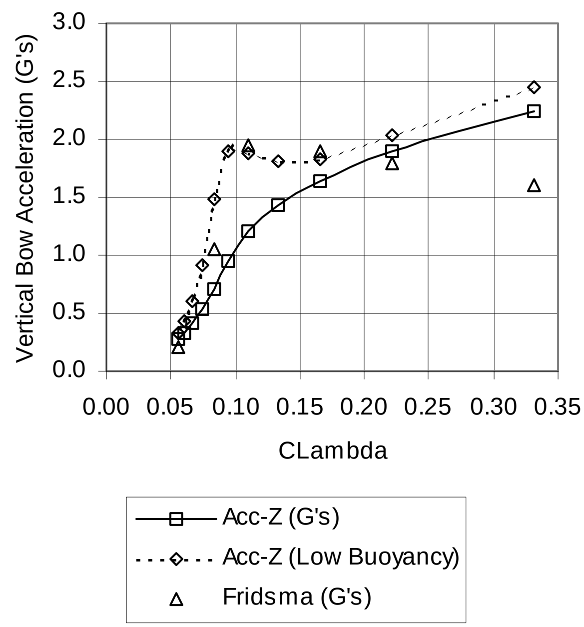

Figure 13 Config.G (24 lb, β=20): Vertical Acceleration at Bow

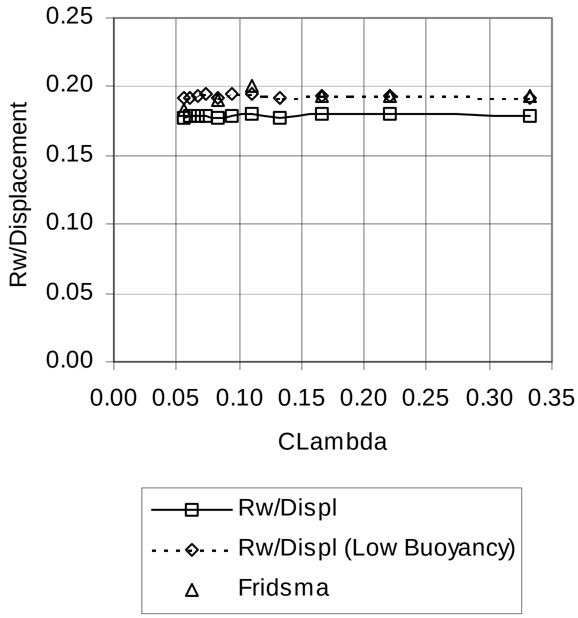

Figure 14 Config.G (24 lb, β=20): Resistance in Waves

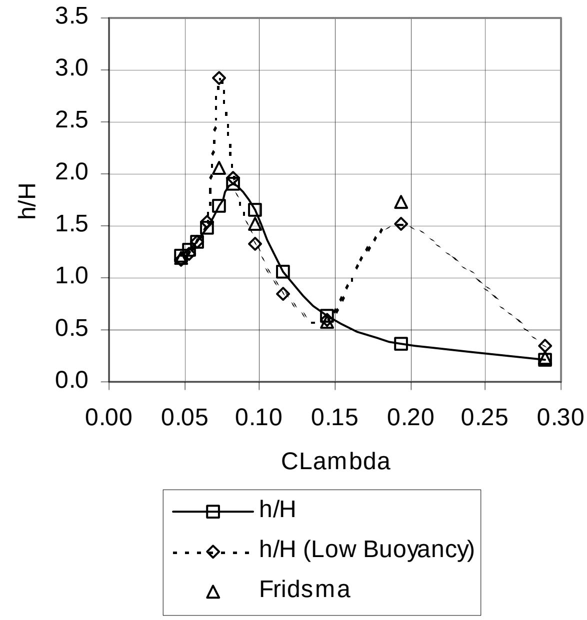

Figure 16 Config.J (16 lb, β=10): Heave Response

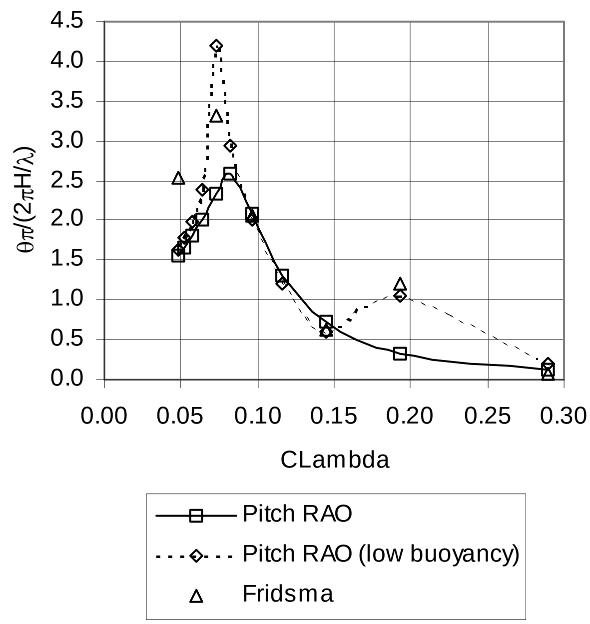

Figure 15 Config.J (16 lb, β=10): Pitch Response

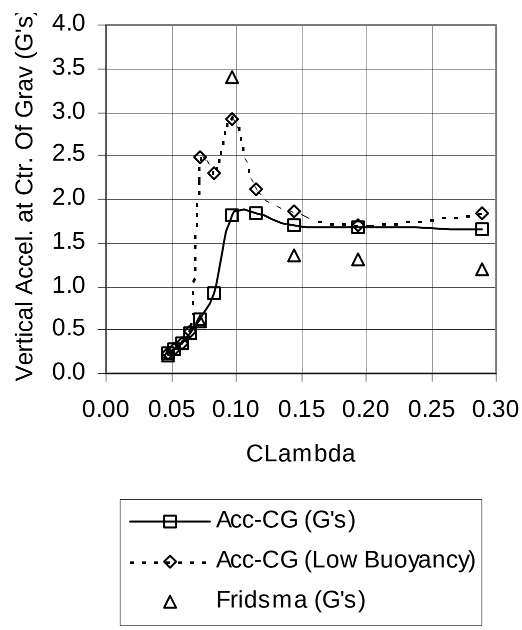

Figure 17 Config.J (16 lb, β=10): Vertical Acceleration at Center of Gravity

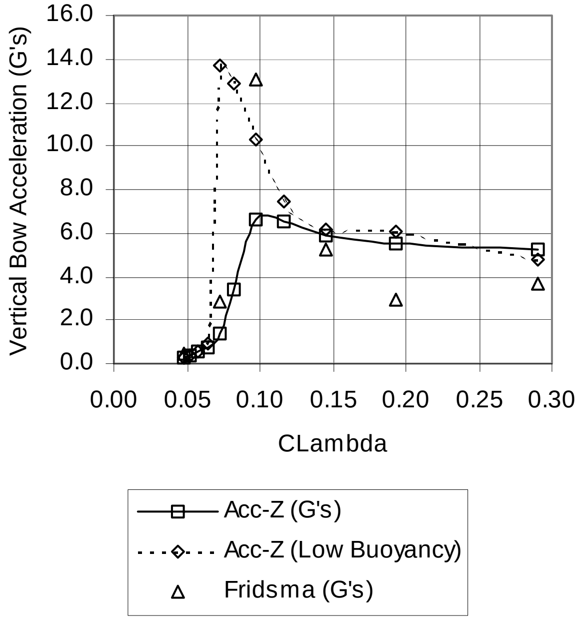

Figure 18 Config.J (16 lb, β=10): Vertical Acceleration at Bow

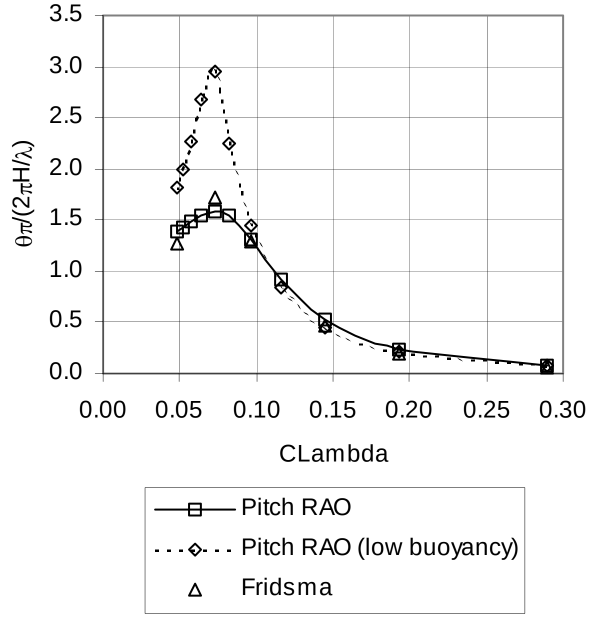

Figure 20 Config.M (16 lb, β=30): Pitch Response

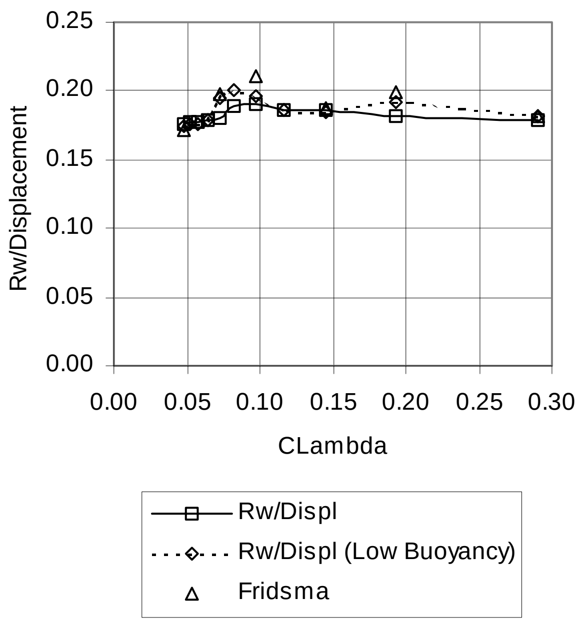

Figure 19 Config.J (16 lb, β=10): Resistance in Waves

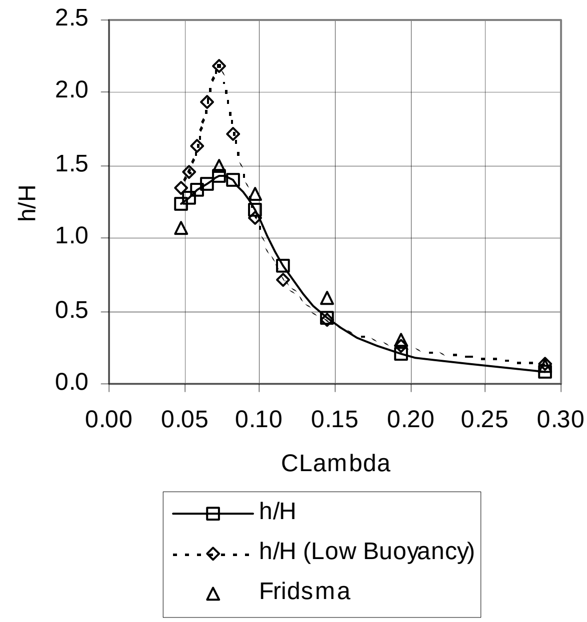

Figure 21 Config.M (16 lb, β=30): Heave Response

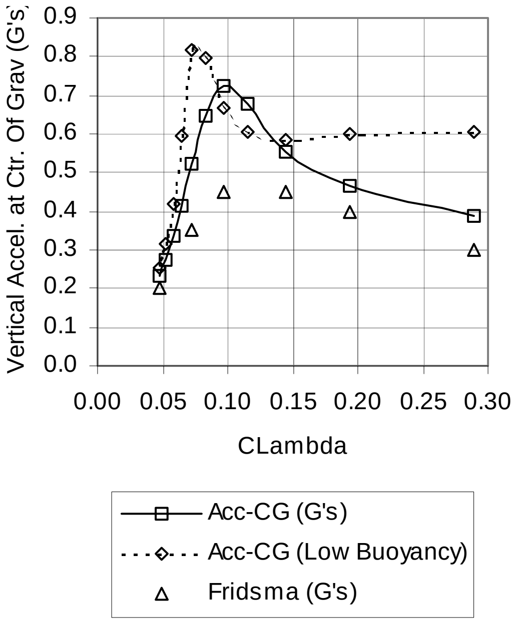

Figure 22 Config.M (16 lb, β=30): Vertical Acceleration at Center of Gravity

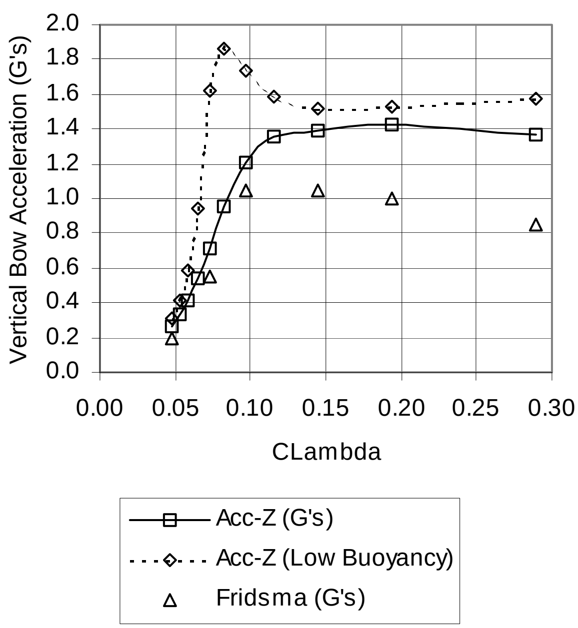

Figure 23 Config.M (16 lb, β=30): Vertical Acceleration at Bow

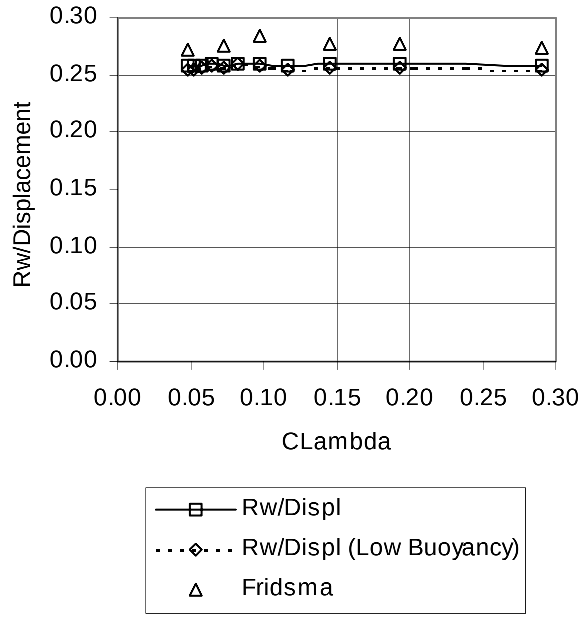

Figure 24 Config.M (16 lb, β=30): Added Resistance in Waves

Validation in Irregular Seas

Fridsma (1971) collected data on the performance of his idealized prismatic models in irregular seas. A limited set of comparisons was made between Fridsma's data and the results of equivalent POWERSEA simulations. In Table 5 conditions 1 and 2 refer to models that are the same hullform as configuration B discussed in the previous section. The model of condition 3 has the same hullform as configuration J in the previous section. All models were tested at a forward speed of 19.611 feet/second, which corresponds to a speed-length ratio of 6.0.

Condition	**1**	**2**	**3**
β (degr)	20	20	10
LCG (%L from bow)	64.0	64.0	68.0
H_{SIG}/B	0.222	0.444	0.444

Table 5 Conditions for Irregular Sea Response Tests

A set of 64 spectral wave components with random phase angles was synthesized for each condition sea state, and each condition was simulated until the vessel encountered approximately 100 waves. A sample of the pitch response to a synthesized wave-train is shown in Figure 25.

The crests and troughs of the heave, pitch and accelerations (at the CG and at the bow) were collected. Heave results were normalized by the significant wave height H. Fridsma chose to display his data in terms of the probability of exceeding a certain peak crest or trough. In Table 6, Table 7 and Table 8 the columns labeled "Probability<50%" means that the probability of a crest exceeding the table value (or a trough being less than the table value) is less than 50%.

	Probability < 50%		Probability < 90%	
	Fridsma	PWRS	Fridsma	PWRS
Heave (h/H)				
Min	-0.036	-0.032	-0.076	-0.061
Max	0.034	0.033	0.067	0.073
Pitch (degrees)				
Min	-0.880	-1.135	-1.780	-2.117
Max	0.900	1.017	2.130	2.063
			Fridsma	PWRS
Ave Peak Vert Accel, CG (G's)			0.680	0.504
Ave Peak Vert Accel, Bow (G's)			2.100	1.492

Table 6 Response to Irregular Sea, Condition 1

	Probability < 50%		Probability < 90%	
	Fridsma	PWRS	Fridsma	PWRS
Heave (h/H)				
Min	-0.145	-0.123	-0.393	-0.242
Max	0.140	0.149	0.255	0.291
Pitch (degrees)				
Min	-2.200	-3.106	-4.340	-5.540
Max	2.250	2.503	5.510	4.557
			Fridsma	PWRS
Ave Peak Vert Accel, CG (G's)			1.77	1.039
Ave Peak Vert Accel, Bow (G's)			5.33	3.571

Table 7 Response to Irregular Sea, Condition 2

	Probability < 50%		Probability < 90%	
	Fridsma	PWRS	Fridsma	PWRS
Heave (h/H)				
Min	-0.135	-0.125	-0.424	-0.224
Max	0.132	0.110	0.259	0.287
Pitch (degrees)				
Min	-2.360	-2.817	-4.870	-4.579
Max	2.390	2.085	5.780	4.165
			Fridsma	PWRS
Ave Peak Vert Accel, CG (G's)			2.40	1.570
Ave Peak Vert Accel, Bow (G's)			7.20	5.238

Table 8 Response to Irregular Sea, Condition 3

For all three conditions the heave and pitch response correlated well with Fridsma's measurements, especially at the 90% probability. The algorithm under predicted the average peak vertical accelerations at the center of gravity by an average of 34%, and under predicted the acceleration at the bow by an average of 30%

After further analysis, it is possible that the algorithm could be calibrated with respect to a vessel's midship deadrise angle so that accelerations could be predicted accurately for an arbitrary vessel.

In summary, the heave and pitch motion is reproduced accurately with the strip-theory algorithm, while the vertical accelerations are under predicted by 30% to 34%.

STRUCTURAL DESIGN OF PLANING HULLS USING STRIP THEORY

A major problem in the design of high-speed planing craft is predicting the panel loads for structural analysis. There are a number of well known methods for predicting the stress in panels as a function of the applied load, but it is very difficult to predict the loads for given sea state.

Spencer (1975) proposed a methodology for structural design of aluminum crewboats. Since crewboats are essentially prismatic at their operating speed for which the warped forward sections are out of the water, Spencer used Savitsky's method (1964) to predict the trim angle of the vessel, data from Fridsma (1971) to predict the peak accelerations, and a technique proposed by Heller and Jasper (1960) to predict panel pressures. Given the panel pressures, it is well understood how to specify frame spacings and panel thicknesses. This method is widely used and is an historical basis for the dynamic pressure portion of the US Coast Guard's Navigation and Vessel Inspection Circular No. 11-80 (NVIC, 1980).

Predicting Panel Pressures Using Strip-Theory

The force formulas used in the equations of motion can be modified to predict sectional forces. Using the same derivation for the normal force F_N as derived earlier, but avoiding the integration-by-parts substitution for $\int_l m_a \frac{\partial UV}{\partial \xi} d\xi$ yields the following:

$$
\begin{aligned}
F_N = & -M_a \cos(\theta)\ddot{z}_{CG} - M_a \sin(\theta)\ddot{x}_{CG} + Q_a\ddot{\theta} \\
& + M_a\dot{\theta}\left(\dot{z}_{CG}\sin(\theta) - \dot{x}_{CG}\cos(\theta)\right) \\
& + \int_l m_a \frac{dw_Z}{dt}\cos(\theta)d\xi - \int_l m_a w_Z \dot{\theta}\sin(\theta)d\xi \\
& - \int_l m_a V \frac{\partial w_Z}{\partial \xi}\sin(\theta)d\xi + \int_l m_a U \frac{\partial w_Z}{\partial \xi}\cos(\theta)d\xi \\
& + \int_l UV \frac{\partial m_a}{\partial \xi}d\xi - \int_l m_a U\dot{\theta}d\xi \\
& - \int_l m_a U \frac{\partial w_Z}{\partial \xi}\cos(\theta)d\xi + \int_l m_a V \frac{\partial w_Z}{\partial \xi}\sin(\theta)d\xi \\
& - \int_l V\dot{m}_a d\xi - \rho\int_l C_{D,c} b V^2 d\xi
\end{aligned}
$$

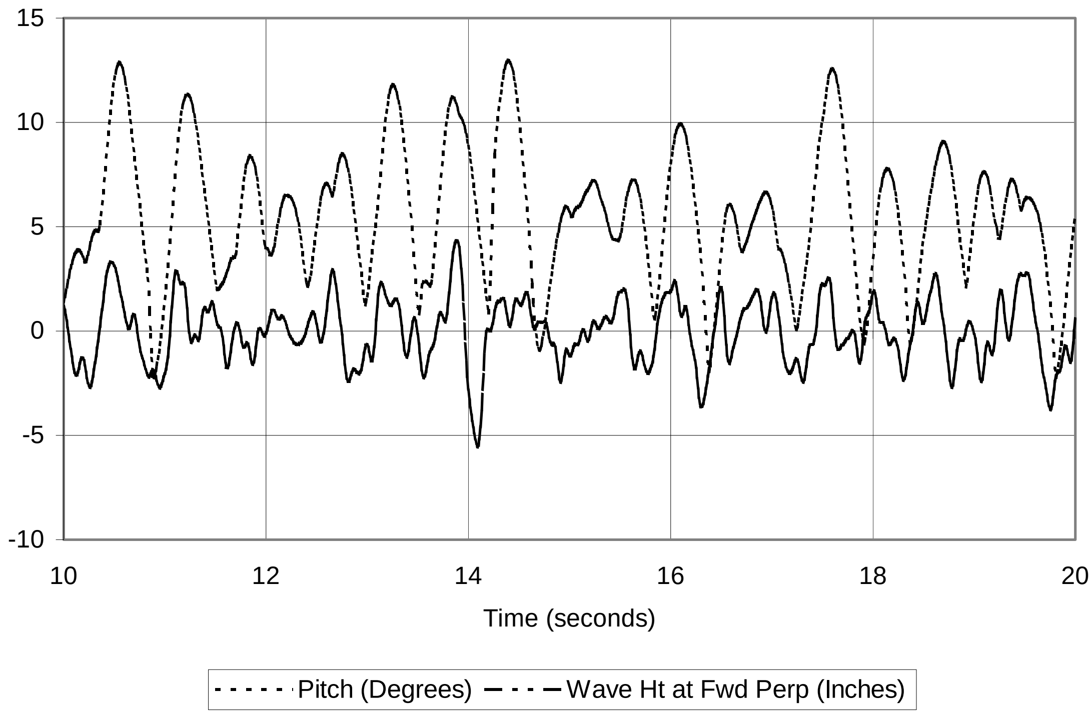

Figure 25 Pitch Response in Irregular Seas (H_{SIG}=0.5 Feet)

Combining terms, replacing the total added mass with the equivalent integral of sectional added masses, and doing the same for the sectional moment of inertia yields:

$$
\begin{aligned}
F_N = & -\int_l m_a \cos(\theta)\ddot{z}_{CG}\,d\xi - \int_l m_a \sin(\theta)\ddot{x}_{CG}\,d\xi \\
& + \int_l m_a \xi\ddot{\theta}\,d\xi + \int_l m_a \dot{\theta}\left(\dot{z}_{CG}\sin(\theta) - \dot{x}_{CG}\cos(\theta)\right)d\xi \\
& + \int_l m_a \frac{dw_Z}{dt}\cos(\theta)\,d\xi - \int_l m_a w_Z \dot{\theta}\sin(\theta)\,d\xi \\
& + \int_l UV\frac{\partial m_a}{\partial \xi}\,d\xi - \int_l m_a U\dot{\theta}\,d\xi \\
& - \int_l V\dot{m}_a\,d\xi - \rho\int_l C_{D,c} b V^2\,d\xi
\end{aligned}
$$

Combining all terms into a single integral over the boat length l, a sectional hydrodynamic normal force can be calculated as:

$$
\begin{aligned}
f_N = & -m_a\cos(\theta)\ddot{z}_{CG} - m_a\sin(\theta)\ddot{x}_{CG} \\
& + m_a\xi\ddot{\theta} + m_a\dot{\theta}\left(\dot{z}_{CG}\sin(\theta) - \dot{x}_{CG}\cos(\theta)\right) \\
& + m_a\frac{dw_Z}{dt}\cos(\theta) - m_a w_Z\dot{\theta}\sin(\theta) \\
& + UV\frac{\partial m_a}{\partial \xi} - m_a U\dot{\theta} \\
& - V\dot{m}_a - \rho C_{D,c} b V^2
\end{aligned}
$$

The total normal force is $F_N = \int_l f_N\,d\xi$.

In the POWERSEA program the term $\frac{\partial m_a}{\partial \xi}$ is calculated using numerical derivatives. Although this introduces a minor inaccuracy in the calculation, this approximation is sufficient for estimating panel pressures. The overall boat motion calculations do not use this approximation. The acceleration terms $\ddot{x}_{CG,}$ $\ddot{z}_{CG,}$ and $\ddot{\theta}$ are estimated using a numerical technique based on a running interpolation-polynomial estimate of state variable derivatives.

The maximum panel pressures are estimated by:

- Running a time-domain simulation on the vessel running at the design load and speed in a synthesized irregular sea, and
- Post-processing the simulation results to find the average of the peak panel pressures for the given panel geometry, speed and sea state.

At each time-step the POWERSEA strip-theory algorithm calculates the wetted beam, hydrodynamic force, and hydrostatic buoyancy at each hydrodynamic section. The hydrodynamic force and hydrostatic buoyancy are combined into a total sectional normal force by the equation $f_T = f_N + \cos(\theta) * f_B$. This force is applied to a strip with an area of a = $B_W * \Delta x$, where B_W is the wetted beam and Δx is the longitudinal strip width. The average pressure on this strip is f_T/a.

A panel pressure for a panel with arbitrary coordinates can be calculated by including a fraction of

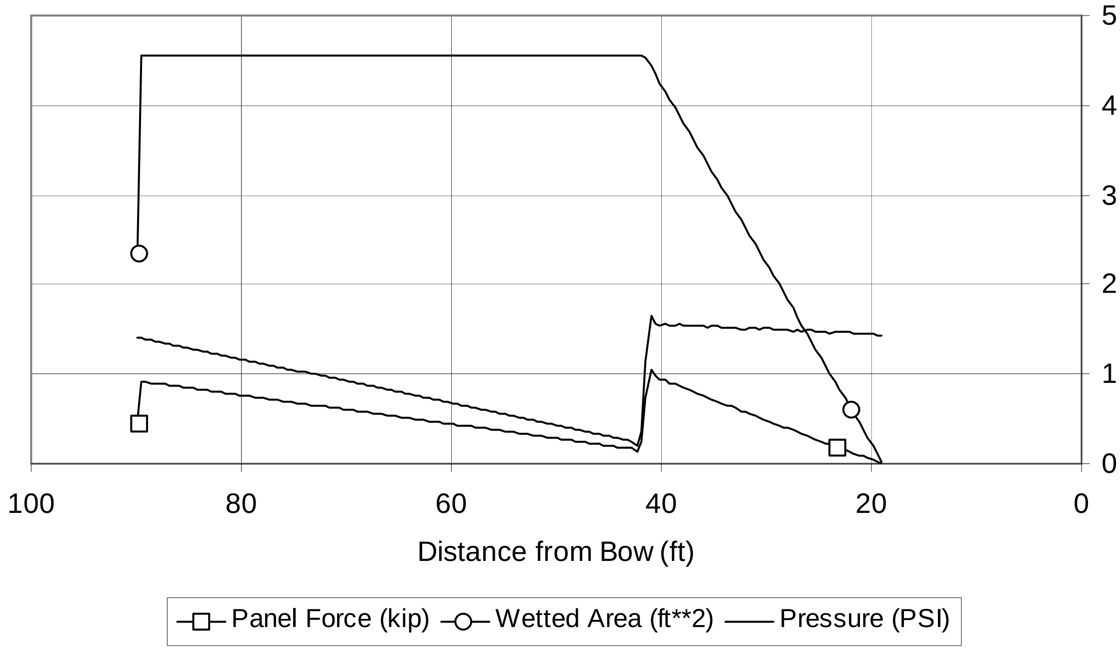

Figure 26 85-foot Crewboat, 30 knots, Quasi-Static Operation. Sectional Wetted Surface, Sectional Normal (Panel) Force and Panel Pressure from POWERSEA Strip Theory Algorithm. Strip theory model includes 201 sections spaced evenly at 0.45 feet per section

the total force for each hydrodynamic section covered by the panel and then dividing by the total area of the panel.

The POWERSEA program is used to simulate vessel motion in a random seaway and collect the peak panel pressures. The average of the 1/10 highest crests is used to estimate the maximum pressure likely to be encountered in an episode of 1000 waves. Although panel pressures are not symmetric about their mean value, a standard engineering assumption is that crests of the pressure can be described in terms of a Rayleigh distribution. It can be shown that in a process described by a Rayleigh distribution the maximum expected crest in an episode of 1000 waves is:

$$\tilde{p}_{1/1000} = 1.46 * \overline{p}_{1/10}$$

where $\overline{p}_{1/10}$ = Ave. of 1/10 highest pressures

and $\tilde{p}_{1/1000}$ = Most probable peak pressure

The most probable peak pressure is a mean transverse pressure. Many investigators have studied transverse pressure distributions on impacting wedges. Vorus (1996) suggests that a transverse pressure distribution for a 20-degree deadrise hull has the following approximate characteristics:

- Minimum value about 10-20% below the mean value
- Maximum value about twice the mean value

Given these observations, a prudent engineering approximation is to use a design pressure that is twice the most probable peak pressure.

Panel Pressures in Structural Design

Design pressures calculated by using the POWERSEA strip-theory algorithm will be compared with design pressures calculated using Spencer's algorithm.

A model of an 85-foot LWL crewboat was created with the characteristics listed in Table 9. The strip theory model consisted of 201 hydrodynamic sections evenly spaced at 0.45-foot intervals over 90-feet LOA. The model was simulated in calm water at a forward speed of 30 knots (beam Froude number of 2.0) using the POWERSEA strip-theory algorithm. Sectional force data was collected and post-processed to obtain the wetted beam, total sectional normal force and panel pressure. The results are plotted in Figure 26. From this figure the keel is wet about 19 feet aft of the bow, and the chines are wet 42 feet aft of the bow

As can be seen in Figure 27, the two algorithms match well at high speeds, while Savitsky's method predicts higher resistance at lower speeds.

The design was modeled with the POWERSEA strip-theory time-domain simulator. Since Spencer recommended using the Savitsky long form method to predict the running trim angle, the POWERSEA model was calibrated to minimize the difference between the trim and resistance results from the strip-theory algorithm and Savitsky's long form method. It was found that setting the buoyancy force coefficient C_{BF} to 0.7 while leaving the buoyancy moment coefficient C_{BM} at 0.5 produced acceptable results.

LOA	90.0	feet
LWL	85.0	feet
Displacement	75	long tons
Average Deadrise	16	degrees
Full Load Draft	3.75	feet
Length/Beam	4.2	
LCG	9%	Abaft Amidships

Table 9 85-foot Crewboat Example

To verify that the strip-theory algorithm produces answers that approximate the Savitsky data used by Spencer in his analysis, a speed-power curve was created using both methods. The results are shown in Figure 27.

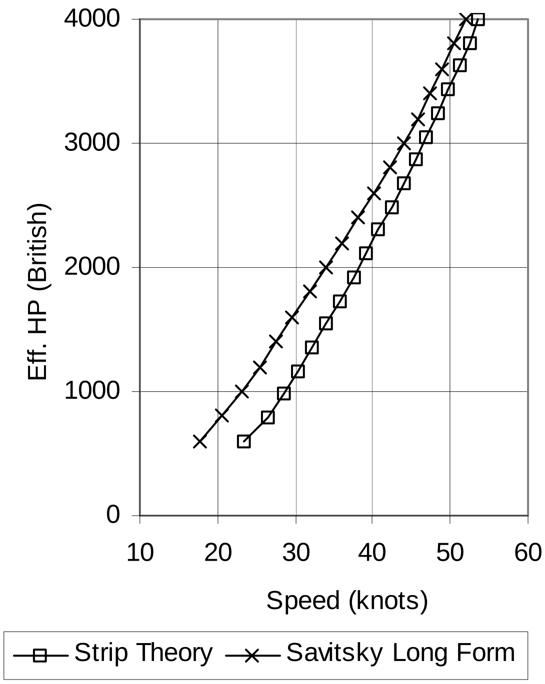

Figure 27 Speed-Power Analysis, 85-Crewboat

There are two reasons for the low-speed discrepancy. First, Savitsky's method is based on data for beam-Froude numbers greater than 2.0 which corresponds to a speed greater than 30 knots for this vessel. Second, for speeds less than 30 knots Savitsky's method predicts a keel wetted length such that the forward, highly-warped sections of the hull are wet. The strip theory algorithm takes the hull warp into account, while Savitsky's long form method does not.

Figure 28 shows the running trim angles predicted by the strip theory algorithm and Savitsky's method as a function of speed. At 30 knots the pitch angle predicted by the two methods differs by about 25%, and the faster the vessel the better the correlation between the two methods.

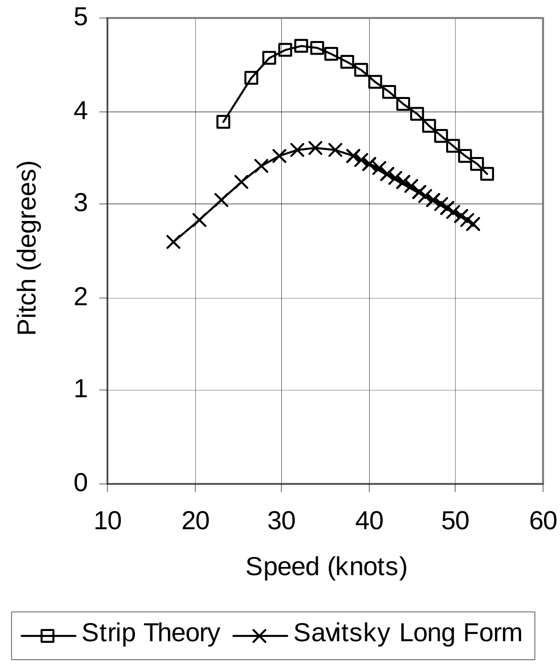

Figure 28 85-foot Crewboat, Trim Angle Predicted by Strip Theory and Savitsky's Long Form Method

Sectional force data was collected for this crewboat operating in a fully-developed random sea with a significant wave height of LWL/12:

H_{SIG} = 7.08 feet

The POWERSEA simulation length was set so that the vessel would encounter roughly 100 waves under these conditions. The random sea algorithm implemented in POWERSEA actually synthesized a sea state with a calculated significant wave height of H_{SIG} = 6.813 feet, a relatively minor discrepancy.

Test panels having a width of 0.1 feet and spanning no more than two hydrodynamic sections were defined at the keel of each station. Narrow panels were used to make sure that the entire panel was wet during the simulation. If wider panels were used the leading edge of the wetted surface might cut through the panel, lowering the mean pressure for that panel. The pressure calculated for each of these panels is shown in Figure 29.

In this example the design pressure at Station 3 and at Station 5 will be calculated. These stations are far enough forward that they will see significant slamming forces, but far enough aft that the keel will be wet during the entire analysis. As can be seen in Figure 29, the average of the 1/10 highest pressures likely to be encountered at Station 3 is 7.6 psi and the pressure at Station 5 is 5.4 psi.

These pressures represent the average of the 1/10 highest pressures, but are not the expected maximum pressures. The expected maximum at Station 3 is:

$$\tilde{p}_{1/1000} = 1.46 * \bar{p}_{1/10} = 1.46 * 7.6 = 11.1 \text{ psi}$$

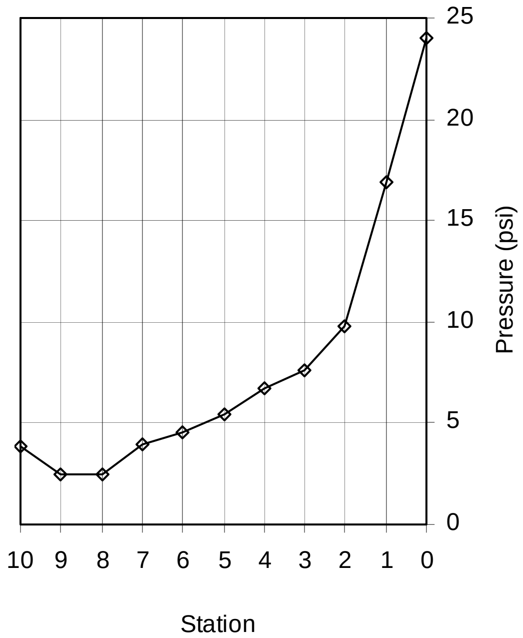

Figure 29 85-foot Crewboat, Simulated Pressure at Keel, Average of 1/10 Highest Crests

The expected maximum at Station 5 is 7.9 psi. Given that the expected pressures are proportional to the vessel's accelerations, and that the POWERSEA strip-theory algorithm under predicts acceleration by 30% to 34%, a reasonable engineering assumption is that the panel pressures should be increased by 30% to 34%. Using 34% yields a panel pressure of 14.9 psi at Station 3 and 10.6 psi at Station 5.

Multiplying these by a factor of two to approximate the peak transverse pressure results in a design pressure of 29.8 psi at Station 3 and 21.2 psi at Station 5.

Comparison with Method of Spencer

Spencer suggested that an impact pressure for a particular panel could be calculated using an empirical equation that relates vessel particulars to impact pressure:

$$P_i = 6.4 + 6.32\, \Delta_{LT}^{1/3} - 0.09\, L + 0.023\, V_K^2 - 0.563\, (V_K\, L)^{1/2}$$

In this example $P_i = 17.7$ psi.

Spencer recommended making adjustments to the pressure to account for non-standard length/beam ratios and for the LCG location:

L/B Correction = +2.3%

LCG Correction = +6.9%

P_i then becomes 19.3 psi. Spencer defined an area factor that is a function of the estimated minimum size of the panel. As the panel size decreases the area factor increases until for very small panels the area factor approaches 1.0. In this example arbitrarily small panels will be assumed, so the area factor F = 1.0.

For the design draft the hydrostatic pressure is:

$$P_s = 0.444\, d = 1.7 \text{ psi}$$

Finally Spencer applied an empirical longitudinal distribution factor that estimates the pressure distribution as a function of the station location. The specified panels are located at Station 3 and 5, so the empirical longitudinal distribution factor in both cases is $F_L = 1.0$

The total design pressure estimated by using the method of Spencer is:

$$P = (F_L * F * P_i) + P_s = (1.0)(1.0)(19.3)+1.7 = 21.0 \text{ psi at both Station 3 and 5}$$

A comparison between the results of Spencer's method and the strip-theory algorithm is shown in Table 10.

Station	Spencer's Method	Strip-Theory Method
3	21.0 psi	29.8 psi
5	21.0 psi	21.2 psi

Table 10 Design Pressures

The pressures predicted by the POWERSEA time-domain strip theory algorithm correlate well with Spencer's estimate at Station 5. At Station 3 the strip-theory algorithm predicts a pressure approximately 40% larger than the method of Spencer.

CONCLUSIONS AND AREAS FOR FURTHER INVESTIGATION

Several methods for predicting the performance and motion of planing craft have been discussed. Particular attention has been paid to a low-aspect ratio strip theory proposed by Zarnick (1978, 1979), and extended and implemented in the form of a computer program called POWERSEA. The implementation was validated against test data collected by Fridsma (1969, 1971). The algorithm as implemented predicts heave motion, pitch motion, and calm water resistance quite accurately. For regular and random seas the vertical acceleration at the center of gravity and the vertical acceleration at the bow are under predicted by 30%, although the predicted accelerations are repeatable and can be adjusted for engineering purposes.

An area for further investigation is the incorporation of a more sophisticated added mass model that takes into account the geometric relationship between consecutive sections and also the instantaneous shape of convex or concave sections. The existing theory is based on impacting wedges with constant deadrise transversely, but to be more accurate the model could be extended to support withdrawing wedges as well. Certainly the effective wetted beam of a withdrawing wedge is not the same as that of an impacting wedge.

The low aspect ratio strip theory was extended so that panel pressures could be estimated. The results compare well with those calculated using Spencer's method. The strip-theory algorithm has the major advantage that it can predict the motions and pressures on non-prismatic hulls and hulls with significant non-linearity's such as steps, tabs and other appendages.

The existing pressure theory does not model transverse pressure changes. It is well known that there is a significant transverse pressure gradient, and this gradient could be modeled empirically so as to improve panel pressure predictions.

REFERENCES

FRIDSMA, GERARD 1969 A Systematic study of the Rough-Water Performance of Planing Boats Report 1275, Davidson Laboratory, Stevens Institute of Technology, Hoboken, New Jersey.

FRIDSMA, GERARD 1971 A Systematic study of the Rough Water Performance of Planing Boats (Irregular Waves -- Part II) Report 11495, Davidson Laboratory, Stevens Institute of Technology, Hoboken, New Jersey.

HELLER, S. R. JR., and JASPER, N. H. 1960 On the Structural Design of Planing Craft. *Quarterly Transactions of the Royal Institution of Naval Architects*, July.

MARTIN, M. 1976 Theoretical Predictions of Motions of High-Speed Planing Boats in Waves. David W. Taylor Naval Ship Research and Development Center, DTNSRDC-76/0069.

_, (NVIC) 1980 Structural Plan Review Guidelines for Aluminum Small Passenger Vessel, *Navigation and Vessel Inspection Circular No. 11-80*. U. S. Coast Guard, Washington, D.C.

SAVITSKY, D. 1964 Hydrodynamic Design of Planing Hulls. *Marine Technology*, **1**, 1, 71-95.

SAVITSKY, DANIEL, and BROWN, P. WARD 1976 Procedures for Hydrodynamic Evaluation of Planing Hulls in Smooth and Rough Water. *Marine Technology*, **13**, 4, 381-400.

SHUFORD, CHARLES L. , Jr. 1958 A Theoretical and Experimental Study of Planing Surfaces Including Effects of Cross Section and Plan Form. NACA Report 1355.

SPENCER, JOHN S. 1975 Structural Design of Crewboats. *Marine Technology*, **12**, 3, 267-274.

SYDOW, J., 1938 Uber den Einfluss von Lederung und Kislung auf den Landestoss. *Jarbuch der Deutschen Luftfarhtforschung.*

VORUS, WILLIAM S. 1996 A Flat Cylinder Theory for Vessel Impact and Steady Planing Resistance. *Journal of Ship Research*, **40**, 2, 100.

VON KARMAN', T. 1929 The Impact of Seaplane Floats During Landing. NACA Technical Note TN 321, Washington, D.C.

WAGNER, H. 1932 Uber stoss-und gleitvorgange an der oberflache von flussigkeiten. *Zeitschrift fur Angewandte Mathematik und Mechanik,* Volume 12 (August), page 193.

ZARNICK, ERNEST E. 1978 A Nonlinear Mathematical Model of Motions of a Planing Boat in Regular Waves. David W. Taylor Naval Ship Research and Development Center, DTNSRDC-78/032.

ZARNICK, ERNEST E. 1979 A Nonlinear Mathematical Model of Motions of a Planing Boat in Irregular Waves. David W. Taylor Naval Ship Research and Development Center, DTNSRDC/SPD-0867-01.